

# Anomalous transport in disordered exclusion processes with coupled particles

**Róbert Juhász**

Research Institute for Solid State Physics and Optics, H-1525 Budapest, P.O. Box 49, Hungary

E-mail: [juhasz@szfki.hu](mailto:juhasz@szfki.hu)

**Abstract.** We consider one-dimensional asymmetric exclusion processes with a simple attractive interaction, where the distance between consecutive particles is not allowed to exceed a certain limit and investigate the consequences of this coupling on the transport properties in the presence of random-force type disorder by means of a phenomenological random trap picture. In the phase-separated steady state of the model defined on a finite ring, the properties of the density profile are studied and the exponent governing the decay of the current with the system size in the biased phase is derived. In case all consecutive particles are coupled with each other and form a closed string, the current is found to be enhanced compared to the model without coupling, while if groups of consecutive particles form finite strings, the current is reduced. The motion of a semi-infinite string entering an initially empty lattice is also studied. Here, the diffusion of the head of the string is found to be anomalous, and two phases can be distinguished, which are characterised by different functional dependences of the diffusion exponent on the bias. The obtained results are checked by numerical simulation.

PACS numbers: 05.60.-k, 05.40.-a, 05.70.Ln, 64.75.Gh

## 1. Introduction

In low dimensions, the characteristics of transport in inhomogeneous media may drastically differ from those in homogeneous environment. This is to be seen already for the thoroughly-studied problem of random walk on a one-dimensional lattice with quenched random hop rates [1, 2, 3, 4, 5, 6, 7, 8]. The most striking anomalies are observed when the disorder is of random-force type, i.e. the direction of the local bias is random. In this case, the diffusion is anomalous, characterised by a diffusion exponent continuously varying with the global bias [5, 6], while it becomes logarithmically slow for zero global bias—a phenomenon known as Sinai diffusion [7]. Much less is known for the transport of interacting many-particle systems on disordered one-dimensional lattices. The zero-range process (ZRP) [9, 10], where lattice sites are allowed to be multiply occupied by identical particles, has a product-measure steady state even in the case of random hop rates and it is closely related to the corresponding one-particle problem (random walk) on the same lattice. Beyond ZRP, perhaps the simplest interacting driven many-particle system is the asymmetric simple exclusion process (ASEP)[11, 12], where particles interact by hard-core exclusion. For this model, there are two ways to introduce disorder: random rates can be associated either with particles or with sites (links). The former model, the ASEP with particle-wise disorder [13, 14, 15] can be mapped to a disordered ZRP, whereas for the ASEP with site-wise disorder [16, 17, 18, 19, 20], general exact solutions are not at our disposal. By means of a phenomenological random trap picture, the current of the latter model has been shown to display an anomalous behaviour similar to that of the random walk in the case of random-force type disorder [19].

Hard-core exclusion can be thought of as a simple repulsive interaction between neighbouring particles. One may also consider attractive interactions between particles, the simplest form of which in one-dimension is, analogous to hard-core exclusion, when the distance between consecutive particles is not allowed to exceed a certain value, say,  $l + 1$  lattice spacings ( $l \geq 1$ ), i.e. a string of coupled particles is formed. From the point of view of holes (empty sites), this prescription transforms to the constraint that the size of clusters of holes is at most  $l$ . Regarding the number of holes in front of particle  $i$  as an occupation number on the  $i$ th site of a virtual lattice, the process maps to the so-called generalised exclusion process [11], which is a ZRP with an upper limit  $l$  for the local occupation numbers. Considering *particle-wise* disorder in the model of coupled particles, it transforms to a generalised exclusion process with *site-wise* disorder. For the latter model with random-force type disorder, the scaling form of the current was argued to be independent of  $l$ , thus identical to that of the ASEP, which is the  $l = 1$  limit of the generalised exclusion process [19]. The model of coupled particles with site-wise disorder with  $l = 1$  maps to an exclusion process with double-sized particles with site-wise disorder, however, a similar mapping does not exist for  $l > 1$  [19]. For the process with  $l = 1$  in the presence of random-force type disorder, the dynamical exponent has been found to differ from that of the ASEP [19].

The aim of this paper is to study the exclusion process with coupled particles in the presence of site-wise random-force type disorder for general  $l$  and to explore, in which extent the transport properties are modified compared to the ASEP by the simple attractive interaction introduced above, which breaks particle-hole symmetry. We shall investigate the distribution of the sample-dependent current and the properties of the density profile in the non-equilibrium steady state on a finite ring, as well as non-stationary phenomena such as the diffusion of a semi-infinite string by means of a phenomenological random trap model and numerical simulation.

Beside theoretical interest, another source of motivations is the applicability of simple variants of exclusion processes to the description of transport phenomena in a large variety of real systems such as vehicular traffic [21] or various biological transport processes [22]. Concerning the latter, random-force type disorder may emerge in several contexts such as DNA unzipping [23], translocation of RNA or DNA through pores [24] or motion of molecular motors [25] on heterogeneous tracks [26, 24]. In many cases, molecular motors act in groups and the collective effects have been studied in different models [27], including models with hard core repulsion [28] or elastic coupling [29] between particles moving in a periodic potential. Our simple model may serve as a ground for testing the joint effect of hard-core repulsion, coupling and disorder in such model systems. A more direct example is served by a recent work, in which the diffusion of finite strings of coupled particles on a homogeneous one-dimensional lattice has been studied [30], motivated by the modelling of synthetic molecular systems, known as molecular spiders, which can move on surfaces and tracks [31]. The model to be studied here may thus be relevant for investigating the influence of track heterogeneity on the transport properties of these systems.

The rest of the paper is organised as follows. In Sec. 2, the model to be studied is defined. In Sec. 3, the properties of closed strings are investigated on finite rings and the results are formulated generally in Sec. 4. In Sec. 5, the problem of diffusion of a semi-infinite string is discussed, while Sec. 6 is devoted to problems concerning the traffic of finite strings, including the steady state and the invasion. Finally, the paper is closed with a discussion of the results in Sec. 7.

## 2. The model

The process that we focus on in the first part of this work is defined on a ring with  $L$  sites. On this lattice,  $N$  particles, which are numbered consecutively along the chain from left to right, are distributed in such a way that each lattice site is occupied by at most one particle and, in case of a closed string, for the number of empty sites  $h_i$  in front of the  $i$ th particle,  $h_i \leq l$  holds for all  $i$ , while in case of an open string  $h_i \leq l$  is prescribed for all but one particle (the  $N$ th one). Obviously, for the closed string,  $L/(l+1) \leq N$  must hold. In this system, a continuous-time Markov process is considered, in the course of which particles attempt to change their positions independently and randomly. The allowed transitions are the following: The  $i$ th particle on site  $j$  attempts to hop to the

adjacent lattice site on its right-hand side with a site-dependent rate  $p_j$ , and the trial is successful if  $h_i \geq 1$  and  $h_{i-1} < l$ . Here,  $h_0 \equiv h_N$  and for particle 1 of an open string, the condition  $h_N < l$  is cancelled. Particle  $i$  on site  $j$  hops to the adjacent site on its left-hand side with a site-dependent rate  $q_j$ , provided  $h_{i-1} \geq 1$  and  $h_i < l$ . For the  $N$ th particle of an open string, the condition  $h_N < l$  is ignored again. The hop rates  $p_j$  and  $q_j$  are independent, identically distributed quenched random variables drawn from the distributions  $\rho(p)$  and  $\pi(q)$ , respectively. Introducing the potential difference between site  $i$  and  $i - 1$  through the relation

$$\Delta U_i \equiv \ln(q_i/p_{i-1}), \quad (1)$$

the average decrease of the potential per lattice spacing  $F \equiv -\overline{\ln(q/p)}$  can be regarded as an average force which the particles are subjected to. Here and in the rest of the paper, the overbar stands for the average over  $\rho(p)$  and  $\pi(q)$ . Without loss of generality, we assume  $F \geq 0$ , i.e. there is either an average bias to the right or the system is unbiased and we restrict ourselves to randomness distributions where the fraction of sites with  $p_j < q_j$  is finite. The natural control parameter  $\mu$  of the one-particle problem, which we retain also for the many-particle process, is given by the positive root of the equation (for  $F > 0$ )[4]:

$$\overline{\left(\frac{q}{p}\right)^\mu} = 1. \quad (2)$$

It is monotonously increasing with  $F$  and zero in the unbiased case ( $F = 0$ ). In the numerical simulations, we used a bimodal distribution for the hop rates, where  $p_i q_i = r$  holds for all  $i$  and the distribution of forward hop rates  $p_i$  is given by

$$\rho(p) = c\delta(p - r) + (1 - c)\delta(p - 1), \quad (3)$$

with the parameters  $0 \leq r \leq 1$  and  $0 < c \leq 1/2$ . For this distribution, the average bias is zero if  $c = 1/2$  and the control parameter reads as

$$\mu = \frac{\ln(1/c - 1)}{\ln(1/r)}. \quad (4)$$

### 3. Steady state of a closed string

We start our investigations by analysing the stationary properties of a finite closed string. In general, we are interested in the scaling behaviour of various quantities in the large  $L$  limit, when the global density of particles  $N/L$  is kept constant.

With the purpose of studying the model in the presence of an external bias ( $\mu > 0$ ), we invoke the random trap model of the random walk in a biased random-force type environment. This picture is based on the observation that the walker spends long times in certain localised regions (trapping regions) and in between, it performs a more or less directed motion. The process is thus approximated by a directed walk between traps characterised by effective trapping (or waiting) times, the distribution of which is broad [32]. This simplified model proved to describe the large-scale properties of the system

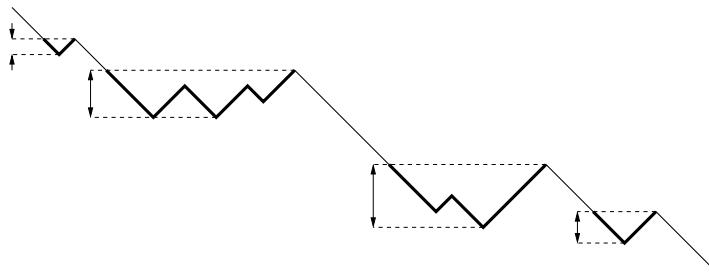


**Figure 1.** Illustration of the potential landscape defined by eq. (1). The trapping regions are indicated by thick lines and the arrows show the heights of the barriers.

correctly [4]. In the potential landscape of the infinite system, defined by eq. (1), which is a descending random walk path with average slope  $-F$  (see Fig. 1), a trapping region can be identified as a basin on the left-hand side of a local maximum at site  $n$  for which  $U_n > U_i$  holds for all sites  $i > n$ . The ascending section of the basin from the minimum to the maximum will be termed barrier. The waiting time  $\tau$  in a trapping region is in the order of the inverse of the persistence probability of a walker starting at the minimum of the basin with an imaginary absorbing site on its left-hand side [19]. This quantity is of the form of a Kesten-variable [33], the distribution of which has an algebraic tail for large  $\tau$ :

$$p(\tau) \sim \tau^{-1-\mu}, \quad (5)$$

where  $\mu$  is given by eq. (2). The waiting time  $\tau$  is related to the potential difference between the maximum and minimum, i.e. the height of the barrier  $U$  as  $\tau \sim e^U$  for large  $U$ . For the ASEP with site-wise disorder, which has been studied in the framework of this simplified model [19], a phase separation can be observed: At the largest barrier, which serves as a bottleneck, a front appears, which separates a macroscopic high-density domain from a macroscopic low-density one and, as a consequence of particle-hole symmetry, the front is located where the potential is half the height of the barrier [34]. For the process under study, the situation is similar: the current is controlled by the largest barrier present in the system, where a front develops, however, as the particle-hole symmetry is broken, half-filling is no longer valid. Therefore, we consider first an isolated barrier of height  $U$  and express the current in terms of the one-particle waiting time.

Let us assume that the front is located at some potential  $bU$  ( $b < 1$ ), which is measured from the bottom of the barrier (see Fig. 2). On the left-hand side of the front the particles sit closely next to each other so that the particle density is nearly 1 (high-density phase), whereas on the right-hand side, particles are as far from each other as possible and the density is close to  $1/(l+1)$  (low-density phase). In case of such a configuration, two kinds of processes which result in the shift of the front may take place: Starting from the front, holes diffuse to the left through the high-density phase and particles diffuse from the front to the right through the low-density phase over the barrier. In fact, the event that a hole detaches from the front and goes away

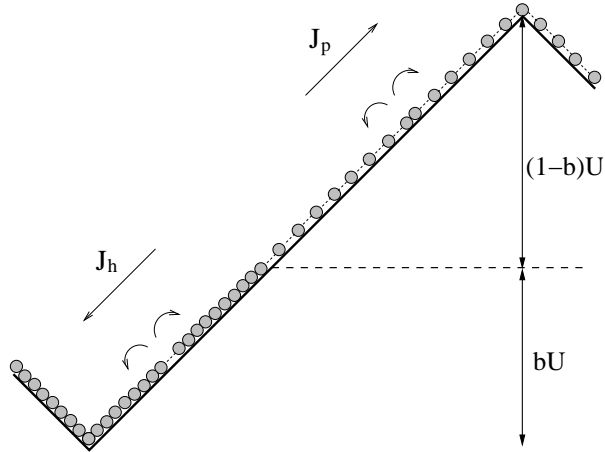


**Figure 2.** Typical configuration of particles at an isolated barrier for  $l = 1$ .

from it is very rare: the probability for this decreases exponentially with the potential difference. Therefore the diffusing holes are practically alone in the high-density phase far from the front and the typical time scale for a hole to successfully overcome the potential barrier  $bU$  and escape to the left is in the order of  $e^{bU}$ . The current of holes in the high-density region is thus  $J_h \sim e^{-bU}$ . The mechanism of particle transport in the low-density phase is similar. Here, particles are immobile since the interparticle spacings are almost everywhere maximal ( $h_i = l$ ). If the particle at the front jumps to the right, a short interparticle spacing with  $h_i = l - 1$  arises in front of this particle and thereby makes it possible for the next particle on its right-hand side, to jump to the right. If the latter event occurs, it can be regarded as if the short spacing moved to the right. For similar reasons as for the holes in the high-density phase, a short spacing is typically by oneself in the low-density phase and moves like a random walker taking steps of length of  $l + 1$  lattice spacings. Thus, in order to escape to the right, this walker has to overcome only a reduced potential barrier  $(1 - b)U/(l + 1)$ . The corresponding time scale is  $e^{(1-b)U/(l+1)}$  and the current of particles through the low-density phase is  $J_p \sim \frac{1}{l+1} e^{-(1-b)U/(l+1)}$ . In the steady state,  $J_h = J_p$  must hold, otherwise the front would move with a finite velocity. This leads to  $e^{-bU} \sim \frac{1}{l+1} e^{-(1-b)U/(l+1)}$  and for large  $U$ , i.e.  $U \gg l \ln l$ , we obtain  $b = 1/(l + 2)$ . The particle current  $j$  at the barrier is thus given by

$$j \sim e^{-U/(l+2)} \sim \tau^{-1/(l+2)} \quad (6)$$

in terms of the one-particle waiting time  $\tau$ .

### 3.1. Current

It is clear that the quantity  $j$  derived above is merely the transport capacity of the barrier, i.e. the maximal current which can flow through it and the actual current is controlled by the incoming current of particles  $j_{in}$  if  $j_{in} < j$ . In a disordered ring of size  $L$ , the stationary current  $J_L$  is determined by the smallest one among the capacities of

barriers present in the system:  $J_L = \min\{j_i\}$ . Making use of eq. (5) and eq. (6), we obtain that the distribution of capacities has a power-law tail  $\rho(j) \sim j^{-1+(l+2)\mu}$  for small  $j$ . The distribution of the sample-dependent current  $J_L$  is thus given by the well-known Fréchet distribution for large  $L$  [35]:

$$p(\tilde{J}) = (l+2)\mu\tilde{J}^{(l+2)\mu-1}e^{-\tilde{J}^{(l+2)\mu}}, \quad (7)$$

in terms of the scaling variable  $\tilde{J} = cJ_L L^{\frac{1}{(l+2)\mu}}$ , where the constant  $c$  is related to the pre-factor in the asymptotical form of  $\rho(j)$ . Thus, the current scales with the system size  $L$  as

$$J_L \sim L^{-\frac{1}{(l+2)\mu}}, \quad (8)$$

and vanishes in the limit  $L \rightarrow \infty$ .

We have performed numerical simulations for finite rings of size  $L = 128, 256, 512, 1024, 2048$  and after waiting sufficiently long time such that the system has settled in a steady state we measured the current. This procedure was then repeated for  $3 \times 10^4$  independent samples for each  $L$ . As can be seen in Fig. 3 and Fig. 4, the Fréchet distribution fits satisfactorily to the distribution of the current, and keeping in mind that the size of the largest trapping region is only  $O(\ln L)$ , the deviations can be assigned to corrections to scaling, which may be still considerable for the numerically available systems sizes.

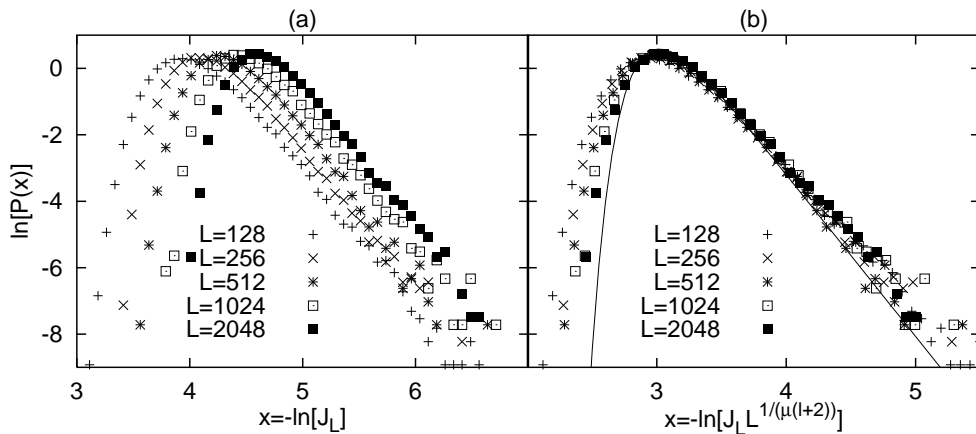


**Figure 3.** a) Distribution of the logarithm of the current measured in numerical simulations for different system sizes in the model with  $l = 2$ . b) Scaling plot of the distributions. The number of particles was  $N = L/2$  and the binary randomness defined in eq. (3) was used with  $c = 0.3$  and  $r = 0.5$ , where the control parameter is  $\mu \approx 1.222$ . The solid curve is the Fréchet distribution given in eq. (7).

Reducing the control parameter, the exponent governing the finite-size scaling of the current is increasing and finally diverges as the unbiased situation is approached, i.e. when  $\mu \rightarrow 0$ . Strictly for  $\mu = 0$ , the random trap approximation breaks down since the size of the largest trapping region is  $O(L)$ . Since the height of the largest barrier is  $O(\sqrt{L})$ , we expect that the magnitude of the current scales typically as  $-\ln |J_L| \sim \sqrt{L}$ .

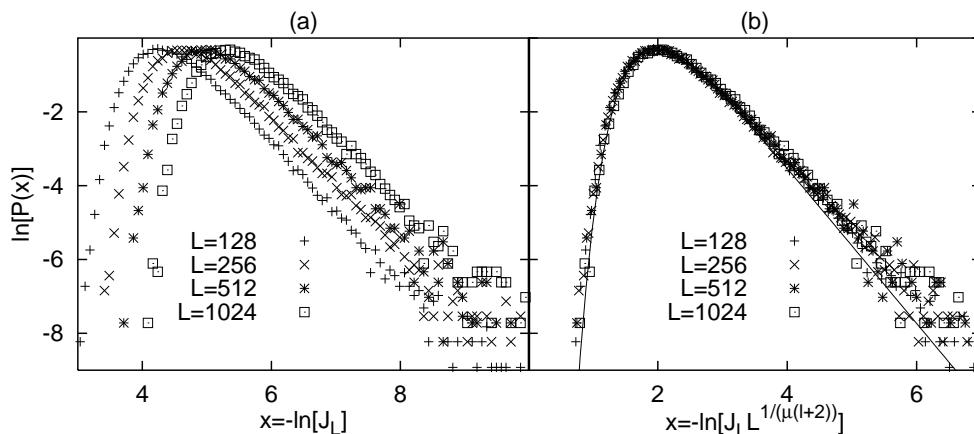


**Figure 4.** a) Distribution of the logarithm of the current measured in numerical simulations for different system sizes in the model with  $l = 2$ . b) Scaling plot of the distributions. The number of particles was  $N = L/2$  and the binary randomness defined in eq. (3) was used with  $c = 0.3$  and  $r = 0.2$ , where the control parameter is  $\mu \approx 0.526$ . The solid curve is the Fréchet distribution given in eq. (7).

As the relaxation time is exponentially large, the dynamics in the unbiased case will be tested numerically in the context of the diffusion of a semi-infinite string in Sec. 5.

### 3.2. Density profile

The steady-state average of the local occupation number  $\nu_i$ , which is zero (one) for empty (occupied) sites, is plotted against the site index  $i$  in Fig. 5 for a given sample. As can be seen, the steady state is segregated: the profile consists of a low-density phase, which extends from site  $\sim 150$  to site  $\sim 320$ , and a high-density phase in the remaining part of the ring. In the low-density phase, the string is stretched out (i.e.  $h_i = l$ ) almost everywhere and this configuration is more or less fixed by the rugged landscape, which results in strong spatial variations in the profile with a period  $l + 1$ . After filtering out this noise (Fig. 5, lower panel), peaks can be observed in the profile, where the local density significantly exceeds the background density  $1/(l+1)$ . Similarly, in the high-density phase gaps with low local density develop. In the following, we shall estimate the number of peaks and gaps and will see that they both grow algebraically with  $L$ , however, with different exponents.

The peaks and gaps are accumulations of particles and holes, respectively, at barriers with sufficiently large one-particle waiting times. First, let us consider a barrier in the low-density phase with a trapping time  $\tau$  and assume that the string is completely stretched out here, i.e. the interparticle spacings are maximal. Recalling the considerations of the previous section, the capacity of the barrier in case of this configuration is in the order of  $\frac{1}{l+1}\tau^{-1/(l+1)}$ . Apparently, this configuration remains stable only if the incoming flow of particles  $J_L$ , which is determined by the largest barrier, does not exceed the capacity of the barrier concerning this configuration. In the opposite case,

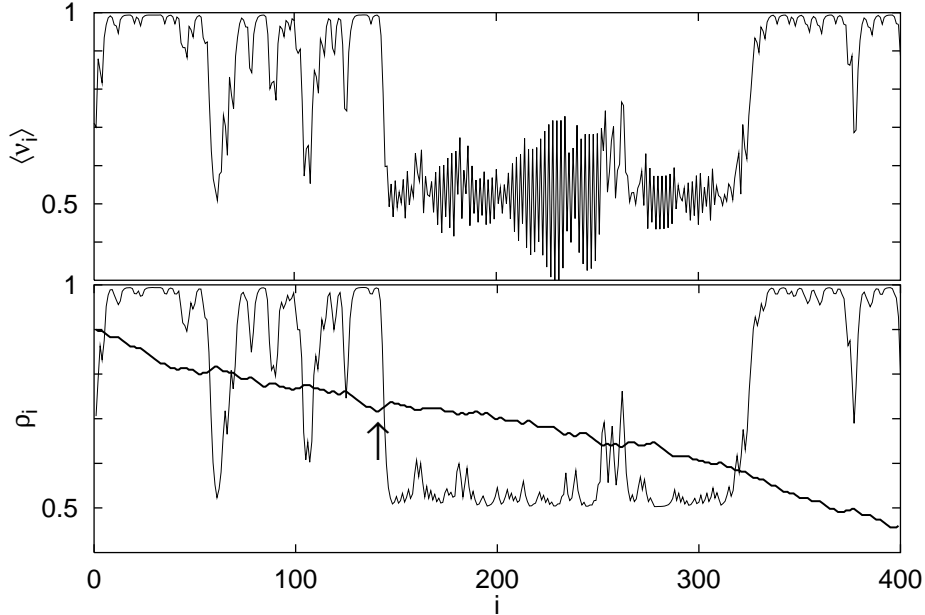


**Figure 5.** Upper panel: Steady-state density profile of the model with  $l = 1$  obtained by numerical simulation in a sample of size  $L = 400$ . The number of particles is  $N = 300$  and the rates were drawn from the bimodal distribution with  $c = 1/3$  and  $r = 1/4$ . Lower panel: Smoothed profile, obtained by averaging over pairs of sites:  $\rho_i = (\langle \nu_i \rangle + \langle \nu_{i+1} \rangle)/2$ . The thick line is the potential landscape defined by eq. (1) and the arrow indicates the starting point of the largest barrier.

particles gradually accumulate here and form a high-density cluster. This process goes on until the front rises up to a certain potential level, so that the capacity concerning this new configuration is identical to the current  $J_L$ . (In this case, the magnitude of the potential at the front measured from the top of the barrier is  $\frac{l+1}{l+2}U$ , where  $U \sim (l+2) \ln(1/J_L)$  is the height of the largest barrier.) We thus expect an accumulation of particles at those trapping regions where  $\frac{1}{l+1}\tau^{-1/(l+1)} < J_L$  holds, or,  $\tau > J_L^{-(l+1)}$  for large  $L$ . The number of barriers of this property is  $N_l \sim L \int_{J_L^{-(l+1)}}^{\infty} p(\tau) d\tau \sim L J_L^{(l+1)\mu}$ , where we made use of eq. (5). Using eq. (8), we obtain for the number of peaks in the low-density phase:

$$N_l \sim L^{\frac{1}{l+2}}. \quad (9)$$

In the high-density phase, the transport is realized by the diffusion of vacancies, and an accumulation, i.e. formation of clusters of  $l$  holes separated by a particle occurs at barriers for which  $\tau > J_L^{-1}$  holds. By a calculation analogous to that carried out for the peaks, we obtain that the number of gaps in the high-density phase is

$$N_h \sim L^{\frac{l+1}{l+2}}. \quad (10)$$

As can be seen, the exponents in eq. (9) and eq. (10) depend only on the parameter  $l$  and are independent of  $\mu$ . In order to check these findings, we have performed numerical

simulations with a global density  $N/L = \frac{l+2}{2(l+1)}$ , so that both the length of the low-density phase and of the high-density phase was  $O(L/2)$ . It was measured in both phases how many times the smoothed steady-state profile intersects the horizontal line at the density  $\frac{l+2}{2(l+1)}$ . The results shown in Fig. 6 are in satisfactory agreement with the theoretical predictions.

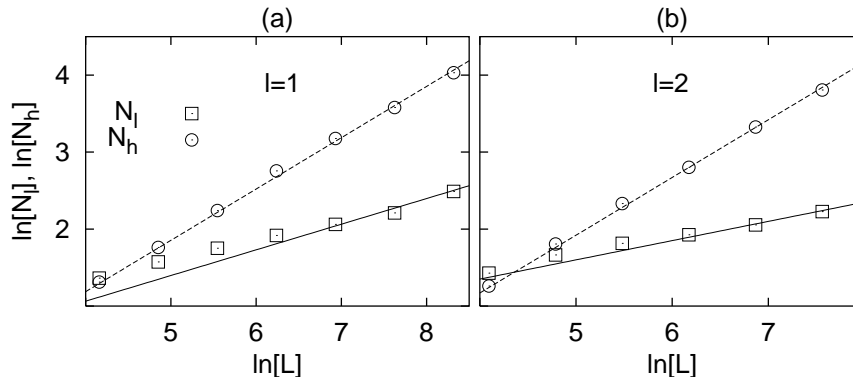


**Figure 6.** Size dependence of the average number of intersections (defined in the text) obtained by numerical simulation for (a)  $l = 1$  and (b)  $l = 2$ . Bimodal randomness was used with  $c = 1/3$  and  $r = 1/4$  and the averaging was performed over  $10^3$  samples. The slope of the solid and dashed lines is  $\frac{1}{l+2}$  and  $\frac{l+1}{l+2}$ , respectively.

### 3.3. Active particles, active holes

In a given time in the steady state, some of the particles reside in the high-density phase and some of them reside in one of the particle clusters (peaks) in the low-density phase. Almost all of these particles are blocked by the hard-core exclusion. Other particles are located in the low-density phase and are blocked since the string is stretched out. All these particles may be termed inactive as they do not contribute to the current. On the other hand, there is a vanishing fraction of particles located between peaks in the low-density phase, which are not blocked by adjacent particles and which are responsible for the transport. In fact, the transport is realized by the diffusion of short interparticle spacings, which we shall call *active particles*. Analogously, in the high-density phase, the current is ascribed to vacancies which diffuse freely between gaps, the so called *active holes*. In the following, we shall estimate the number of active particles and active holes present in the system.

In the high-density phase, the typical distance between adjacent gaps is  $\xi_h \sim L/N_h \sim L^{\frac{1}{l+2}}$ . We will see a posteriori that the concentration of holes in these domains is vanishing, so that they can be regarded as independent walkers. It is known that the motion of a single random walker is controlled by the parameter  $\mu$  [4]. If  $\mu > 1$ , the velocity of active holes is constant, so they pass through the inter-gap region in a time  $t \sim \xi_h$ . The number of active holes  $N_h^a$  present in this domain is related to the current

as  $N_h^a \sim J_L t$ . Using eq. (8), we obtain for the number of active holes between adjacent gaps:  $N_h^a \sim L^{\frac{1-\mu}{l+2}}$ . If  $\mu < 1$ , the diffusion of holes is anomalous, i.e. the travelling time is  $t \sim \xi_h^{\frac{1}{\mu}}$  and the number of active holes between adjacent gaps is independent of  $L$ :  $N_h^a \sim J_L \xi_h^{1/\mu} \sim O(1)$ . The concentration of active holes  $N_h^a/\xi_h$  is thus indeed vanishing for any  $\mu$ .

In the low-density phase, the typical distance between neighbouring peaks is  $\xi_l \sim L/N_l \sim L^{\frac{l+1}{l+2}}$ . The active particles (the short spacings) take steps of length  $l+1$ , therefore their effective waiting time at a barrier is  $\tau^{1/(l+1)}$ . In the asymptotical form of the distribution of this quantity,  $(l+1)\mu$  appears in place of  $\mu$ , thus, we conclude that the motion of active particles is governed by the effective control parameter  $(l+1)\mu$ . If  $\mu > \frac{1}{l+1}$ , the velocity of active particles is finite and we obtain for their number between two adjacent peaks:  $N_p^a \sim J_L \xi_l \sim L^{\frac{l+1}{l+2} - \frac{1}{(l+2)\mu}}$ . If  $\mu < \frac{1}{l+1}$ , we have  $t \sim \xi_l^{\frac{1}{(l+1)\mu}}$  and the number of active particles is independent of  $L$ :  $N_p^a \sim J_L \xi_l^{\frac{1}{(l+1)\mu}} \sim O(1)$ . As can be seen also the concentration of active particles  $N_p^a/\xi_l$  is vanishing.

We have obtained that, as opposed to the number of peaks and gaps, the numbers of active holes and particles depend also on  $\mu$  and the behaviour of the former changes at  $\mu = 1$  while the behaviour of the latter changes at  $\mu = \frac{1}{l+1}$ .

#### 4. General formulation of steady-state results

The results obtained in the previous section are easy to formulate generally for exclusion processes with random-force type disorder, where the active particles and holes responsible for the transport in the low-density and high-density phase (which are not necessarily true particles or holes, as we have seen above) overcome barriers according to the Arrhenius type activated dynamics characterised by a waiting time  $\tilde{\tau}_i \sim e^{f_i U}$ . Here,  $i = 1, 2$  and the index 1 (2) refers to active holes (particles) in the high-density (low-density) phase, and the factors  $f_i$  are characteristic of the particular system. This class of models includes the ASEP, the closed string, the ASEP with large particles [19], the model with finite open strings to be discussed in Sec. 6, and possible combinations of these models.

For models of this class, all the exponents characterising the stationary behaviour of quantities studied in the previous section can be expressed in terms of two exponents:  $\mu_1 = \mu/f_1$  and  $\mu_2 = \mu/f_2$ , which appear in the distribution of effective waiting times  $\tilde{\tau}_i$  of active particles and holes:  $\tilde{p}_i(\tilde{\tau}_i) \sim \tilde{\tau}_i^{-1-\mu_i}$ ,  $i = 1, 2$ . Generalising the argumentations presented in the previous section, one can easily show that the steady state current follows a Fréchet distribution and vanishes according to

$$J_L \sim L^{-\frac{1}{\mu_1 + \mu_2}}. \quad (11)$$

The number of gaps in the high-density phase ( $i = 1$ ) and the number of peaks in the low-density phase ( $i = 2$ ) scales with the system size as

$$N_i \sim L^{1 - \frac{\mu_i}{\mu_1 + \mu_2}}. \quad (12)$$

The typical number of active particles and holes in an inter-barrier domain is

$$N_i^a \sim \begin{cases} L^{\frac{\mu_i-1}{\mu_1+\mu_2}} & \mu_i > 1 \\ O(1). & \mu_i < 1. \end{cases} \quad (13)$$

For the closed string, the basic exponents are  $\mu_1 = \mu$  and  $\mu_2 = (l+1)\mu$ ; for the ASEP,  $\mu_1 = \mu_2 = \mu$ ; and for the exclusion process with particles of size  $d$ , which was studied in Ref. [19],  $\mu_1 = d\mu$  and  $\mu_2 = \mu$ .

## 5. Diffusion of a semi-infinite string

So far, we have studied the steady state properties of the model defined on a ring. Now, we examine how a semi-infinite string moves when it enters an initially empty semi-infinite lattice (see Fig. 7). To be concrete, the string enters at the first lattice site, which means formally that particles are created here with rate 1 and the particle closest to the entrance site is not allowed to jump to the right if it resides at site  $l+1$ . We are interested in the time-dependence of the position  $\overline{\langle x \rangle}$  of the first particle (the head) of the string. Here, the angular brackets denote average over stochastic histories. Let us

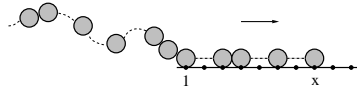


**Figure 7.** Advance of a semi-infinite string.

consider first an isolated barrier of height  $U$  and examine the way the head of the string goes over it.

First, the front of the high-density cluster of accumulated particles is advancing (Fig. 8A) until the head reaches the top of the barrier (Fig. 8B). This process is realized by diffusion of vacancies through the high-density cluster and its time scale is dominated by the escape time of vacancies when the head is in the vicinity of the top, which is  $O(e^U)$ . After the top was reached the head falls over and a stretched segment develops while the front separating it from the high-density segment moves backwards (Fig. 8C). This process, which is realized by the escape of active particles through the stretched segment, goes on until the stable level of the front determined by the incoming current is reached (Fig. 8D). Denoting the potential difference between this level and the maximum by  $U_0$ , the time scale of this process is  $O(e^{U_0/(l+1)})$ . While for  $l > 1$ , the motion of the head is more or less directed after it has fallen over the maximum, for  $l = 1$  a special phenomenon can be observed: The head performs an unbiased random walk and may even return to the top (see Fig. 9). As can be seen from the configurations shown in the figure, the stretched segment is located symmetrically on the two sides of the barrier hence the active particles go over the barrier in both directions with the same rate. Thus, the motion of the head can be described by a symmetric random walk with hop rates  $p(U') = q(U') \sim e^{-U'/(l+1)}$ , which depend on the magnitude of potential

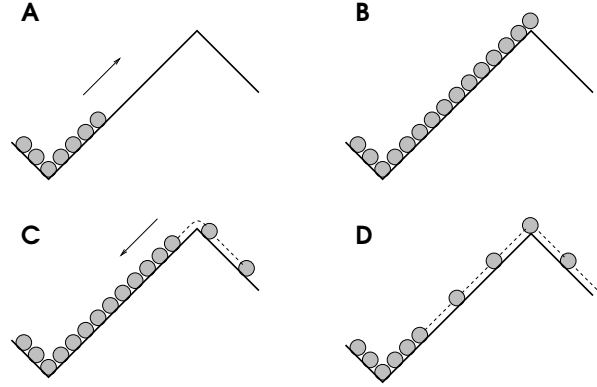


**Figure 8.** The mechanism of overcoming a barrier.

$U'$  (measured from the maximum) at the location of the head. The characteristic time in which the head first reaches a site of potential  $U'$  is in the order of  $e^{U'/(l+1)}$ , see e.g. Ref. [36]. However, during the swinging of the head, vacancies may also escape to the left through the high-density segment. These processes result in the shift of the front and thus induce a bias to the right for the motion of the head. The swinging therefore goes on practically until the front first reaches its stable level and afterwards the motion of the head becomes directed.

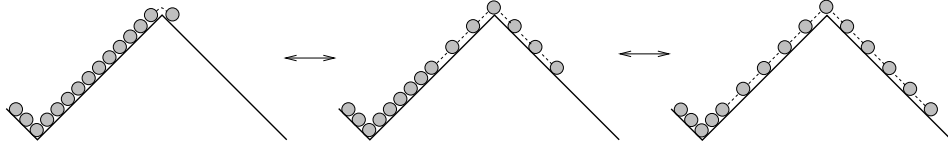


**Figure 9.** The “swinging” of head of the string in the case  $l = 1$ .

We see that the time-determining one among the above steps is the climb of the head to the top of the barrier, the characteristic time of which is in the order of the one-particle waiting time  $e^U$ . It is, however, valid only if the incoming current of particles  $j_{in}$  exceeds  $\tau^{-1}$ . Otherwise the time scale of overcoming the barrier is obviously  $O(\xi/j_{in})$ , where  $\xi$  is the size of the trapping region.

Now, we return to the investigation of the disordered model, where the potential landscape contains barriers of various heights. In what follows, we number the barriers starting from the first site of the lattice and measure distances in terms of the barrier index  $n$ . This can be done since the average distance between the starting points of consecutive barriers is finite. It is clear that  $j_i(l+1)$  is an upper bound for the velocity of the head, where  $j_i$  is the capacity of the largest barrier the head has already left behind. This upper bound obviously changes at such a barrier which is larger than any of the barriers on its left-hand side. The  $m$ th barrier with this property, the so-called  $m$ th *limiting barrier* has a typical distance from the origin  $n_m \sim O(2^m)$  and a typical trapping time  $\tau_m \sim n_m^{1/\mu}$ . Let us consider the  $m$ th limiting barrier, assume that  $m \gg 1$

and estimate the time  $t$  that elapses until, starting from here, the head reaches the next limiting barrier, which is located a distance of  $O(n_m)$  away. As aforesaid, the current of the limiting barrier provides a lower bound  $T_j$  for the travelling time:  $t > T_j \sim \frac{n_m}{j_m^{l+1}}$ . On the other hand, the waiting time of the head at a barrier is at least in the order of the one-particle waiting time, therefore another lower bound is given by the single-particle travelling time:  $t > T_1 \sim \sum_i \tau_i$ . Since the delay of the head at trapping regions and the inflow of particles at the  $m$ th limiting barrier take place simultaneously, we may write  $T_j, T_1 < t < T_j + T_1$  and conclude that the travelling time is composed of two contributions:

$$t \sim O(T_j) + O(T_1). \quad (14)$$

The first term in eq. (14) scales with the distance  $n_m$  as  $T_j \sim n_m^{1 + \frac{1}{(l+2)\mu}}$ . The second term is proportional to  $n_m$  for  $\mu > 1$ , while it is  $T_1 \sim n_m^{1/\mu}$  for  $\mu < 1$ . Comparing the two contributions, we obtain that, for  $\mu > \mu_l^* \equiv \frac{l+1}{l+2}$ , the travelling time is dominated by  $T_j$ , whereas for  $\mu < \mu_l^*$  it is dominated by  $T_1$  for large  $n_m$ . Therefore, inverting these relations, we obtain that the head of the string advances for  $\mu > \mu_l^*$  asymptotically as

$$\overline{\langle x \rangle} \sim t^{\frac{(l+2)\mu}{(l+2)\mu+1}}, \quad (15)$$

while if  $\mu < \mu_l^*$ , we have

$$\overline{\langle x \rangle} \sim t^\mu \quad (16)$$

for large  $t$ . The diffusion of the head is thus anomalous and the diffusion exponent varies continuously with  $\mu$ . At  $\mu = \mu_l^*$  a change occurs in the dependence of the diffusion exponent on  $\mu$  and below this value, the motion of the head follows the diffusion law characteristic of the one-particle problem.

The motion of the head between two limiting barriers is much more complex on a microscopic length scale. At small trapping regions with a waiting time  $\tau_i < j_m^{-1} \sim \tau_m^{-1/(l+2)}$ , the head is delayed until the trapping region is filled up with particles. The release time of the head at large barriers with  $\tau_i > j_m^{-1}$ , the number of which is  $n_m \int_{j_m^{-1}}^{\infty} \tau^{-\mu-1} d\tau \sim n_m \tau_m^{-\mu/(l+2)} \sim n_m^{(l+1)/(l+2)}$ , is  $O(\tau_i)$ . During this time, particles pile up and a queue of length  $\xi_i \sim \tau_m^{-\frac{1}{l+2}} \tau_i$  forms behind such a barrier. After the head was released, its velocity is temporarily determined by the capacity of the barrier instead of that of the true limiting barrier until the (the excess part of the) queue dissolves, which takes a time  $\xi_i/j_i \sim (\frac{\tau_i}{\tau_m})^{\frac{1}{l+2}} \tau_i$ . For the length of the queue behind the  $m+1$ st limiting barrier, we obtain  $\xi_{n_{m+1}} \sim \tau_m^{(l+1)/(l+2)} \sim n_m^{\mu_l^*/\mu}$ . Thus for  $\mu > \mu_l^*$ , the length of the queue piling up behind a limiting barrier until the head is released is typically only a vanishing fraction of the distance from the preceding limiting barrier, while for  $\mu < \mu_l^*$ , the domain behind the head is almost completely filled up with particles. In fact, in the latter case, also queues forming at non-limiting but large barriers may extend to the preceding limiting barrier. The queue temporarily blocks the inflow of particles here, which explains the increase of travelling time of the head compared to that dictated solely by the current of the limiting barrier. We see again from the dynamics of the

queues forming at trapping regions that the properties of the system change at the value  $\mu_l^*$  of the control parameter.

We have performed numerical simulations and measured the time-dependence of the average displacement of the head for different values of the control parameter. Results are shown in Fig. 10. As can be seen, for  $\mu \geq \mu_l^*$ , the diffusion exponent is in good agreement with the predictions. For  $\mu < \mu_l^*$  and for short times, the diffusion seems to follow the law found for  $\mu > \mu_l^*$  (eq. (15)) and for longer times a crossover can be observed to the true asymptotic behaviour (eq. (16)). This means that for short times, the second term in eq. (14) is suppressed by the first one, but ultimately, it dominates the travelling time since it grows with a greater exponent.

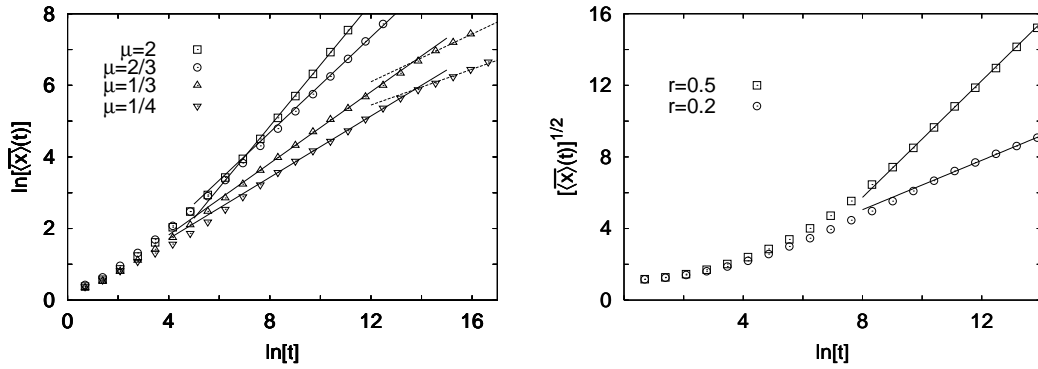


**Figure 10.** Results of numerical simulations. Left panel: the logarithm of the average position of the head plotted against the logarithm of time in the model with  $l = 1$  for different values of the control parameter. Binary randomness was used with parameters  $c = 0.2, r = 0.5$ ;  $c = 0.2, r = 1/8$ ;  $c = 1/3, r = 1/8$ ;  $c = 1/3, r = 1/16$ , where the control parameter takes the values  $\mu = 2, 2/3, 1/3$  and  $1/4$ , respectively. The average was performed over a few hundred independent samples and 3 – 20 runs for each sample. The slope of the solid lines is  $\frac{(l+2)\mu}{(l+2)\mu+1}$ , while that of dashed lines is  $\mu$ . Right panel: Square root of the average position of the head plotted against the logarithm of time in the model with  $l = 1$  in the unbiased case  $\mu = 0$ . The parameters  $c = 0.5$  and  $r = 0.5, 0.2$  were used and the data were averaged over 200 independent samples and 20 runs per sample.

In the limit  $\mu \rightarrow 0$ , the diffusion exponent tends to zero and we expect that for  $\mu = 0$ , the displacement  $\overline{\langle x \rangle}(t)$  grows slower than any power of  $t$ . The unbiased case is out of the scope of the above theory, nevertheless, we can estimate the leading order behaviour of  $\overline{\langle x \rangle}(t)$  by taking into account that the sojourn time  $t$  of a random walker in a domain of size  $\xi$  scales as  $\ln t \sim \sqrt{\xi}$ . Thus, we expect that the average displacement grows as  $\overline{\langle x \rangle}(t) \sim C(\ln t)^2$ , where  $C$  is a non-universal constant. Results of numerical simulations are in accordance with this relation (see Fig. 10).

## 6. Traffic of finite open strings

In the final part of this work, we shall study finite open strings composed of  $m$  particles, which we call shortly  $m$ -strings.

### 6.1. Steady state

First, we are interested in the steady-state properties of systems defined on a ring, in which the density of  $m$ -strings is finite. This model belongs to the model class discussed in Sec. 4, for which the steady-state results presented there are at our disposal once the basic exponents  $\mu_1$  and  $\mu_2$  are known.

In the high-density phase, the active holes which are responsible for the current in the inter-barrier regions are simple holes, consequently, we have  $\mu_1 = \mu$ . In the low-density phase, the active particles are  $m$ -strings moving in the inter-barrier domains. Thus we need the diffusion exponent of an  $m$ -string characterised by the parameters  $m$  and  $l$ . This can be obtained by constructing the network of possible transitions of such systems. Let us consider the simplest case,  $m = 2$ , a “dimer” and denote the state when the left-hand side particle of the dimer is located at site  $i$  and the right-hand side particle at site  $i + 1, i + 2, i + 3, \dots$  by  $A_i, B_i, C_i, \dots$ , respectively. The network of transitions for  $l = 3$  is depicted in Fig. 11 and the corresponding networks for  $l = 2$  ( $l = 1$ ) are obtained by deleting the nodes  $D_i$  ( $D_i$  and  $C_i$ ) and the links connected with them. The conclusions drawn through this example can be easily extended to general

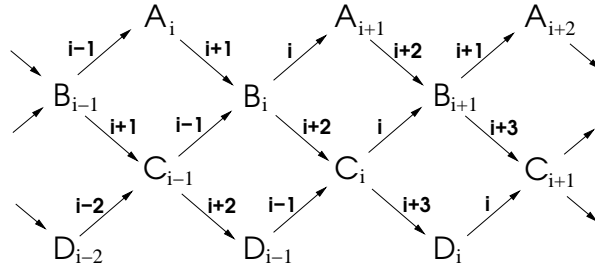


**Figure 11.** Network of transitions for an  $m$ -string with  $m = 2$  and  $l = 3$ . An arrow with index  $i$  symbolises an allowed transition in the direction of the arrow with rate  $p_i$  and in the opposite direction with rate  $q_{i+1}$ .

$m$  and  $l$ . As can be seen, the diffusion of an  $m$ -string can be regarded as a random walk on a disordered quasi-one-dimensional lattice. The walker has several alternative paths to get from one site to another one, however, the potential difference defined by eq. (1) is the same along all paths in an infinite system. Thus, a single-valued potential can be introduced here, just as for a one-dimensional chain. Therefore, when getting from one site to a remote one, the trapping regions cannot be “walked round” and in the point of view of large-scale properties, the existence of alternative paths is irrelevant. Moreover, one can easily make sure that following a path in the network between two distant points, each type of link is contained  $m$ -times in the path. See, for example, the

path  $A_i \rightarrow B_i \rightarrow A_{i+1} \rightarrow B_{i+1} \rightarrow \dots$  in the figure, in which the links of the original lattice are contained doubly. Consequently, the effective height of a barrier felt by an  $m$ -string is  $m$  times greater than the true height. This can also be seen in a more heuristic way by taking into account that one step of an  $m$ -string amounts to  $m$  steps of its constituent particles. Thus, we conclude that  $f_2 = m$  and the exponent governing the diffusion of an  $m$ -string is  $l$ -independent and is given by  $\mu_2 = \mu/m$ . The results in eq. (11)-(13) are thus valid for this model with  $\mu_1 = \mu$  and  $\mu_2 = \mu/m$ . For example, for the finite-size scaling of the current we obtain:

$$J_L \sim L^{-\frac{1}{\mu} \frac{m}{m+1}}. \quad (17)$$

## 6.2. Invasion

In the following, a problem similar to that discussed in Sec. 5 will be examined, i.e. we consider a semi-infinite lattice, which is initially empty, and at the first lattice site  $m$ -strings enter (“invade”) the lattice with a finite entrance rate and we are interested in the advance of the  $m$ -string first entered the system, as well as the evolution of the number of particles on the lattice. Although, the steady-state behaviour could be handled together with the problem of a closed string within a common formalism, the problem of invasion of  $m$ -strings must be treated separately from the diffusion of a semi-infinite string and it has much in common with the invasion of uncoupled particles ( $m = 1$ ), which has been studied in Ref. [19].

From now on, we shall call the  $m$ -strings particles. First, it is clear that the first particle advances with a constant velocity if  $\mu_2 > 1$  ( $\mu > m$ ). Let us assume that  $0 < \mu_2 < 1$  and consider the  $k$ th limiting barrier far from the entrance site, i.e.  $k \gg 1$ , and estimate the travelling time of the first particle between the  $k$ th and the  $k + 1$ st limiting barrier. In this domain, the first particle is caught up by the following particles only at sufficiently large barriers, for which  $\tilde{\tau}_2 > j_k^{-1}$ , where  $j_k \sim n_k^{-1/(\mu_1 + \mu_2)}$  is the current supplied by the  $k$ th limiting barrier. The number of such barriers is  $n_B \sim n_k^{\mu_1/(\mu_1 + \mu_2)}$ . Such a trapping region is filled up with particles in a period of  $O(j_k^{-1})$  to a level at which the escape time of the first particle is in the same order of magnitude,  $O(j_k^{-1})$ . The waiting time of the first particle at such a barrier is thus  $O(n_k^{1/(\mu_1 + \mu_2)})$ . The travelling time of the first particle between two such adjacent barriers, which are located a distance  $\xi_0 \sim n_k/n_B \sim n_k^{\mu_2/(\mu_1 + \mu_2)}$  apart is in the same order of magnitude:  $t_0 \sim \xi_0^{1/\mu_2} \sim n_m^{1/(\mu_1 + \mu_2)}$ . Thus the total travelling time between the  $k$ th and the  $k + 1$ st limiting barrier is  $t \sim n_B n_k^{1/(\mu_1 + \mu_2)} \sim n_k^{(1 + \mu_1)/(\mu_1 + \mu_2)}$ . Inverting this relation, we obtain that the advance of the first particle follows the asymptotic law:

$$\overline{\langle x \rangle} \sim t^{\frac{1+1/m}{1+1/\mu}}, \quad \mu < m. \quad (18)$$

Nevertheless, the average number of particles  $N(t)$  can be shown to grow slower. The number of particles present in the system is approximately equal to the length of the high-density segment, which extends from the entrance site to an advancing front [19]. When the front is located at a limiting barrier in a distance  $N$  from the entrance,

the inflow of particles is controlled by the capacity of this barrier. For the growth rate of  $N$ , we may thus write  $\frac{dN}{dt} \sim N^{-1/(\mu_1+\mu_2)}$ , which yields

$$N(t) \sim t^{\frac{1+1/m}{1+1/m+1/\mu}}. \quad (19)$$

So, the total number of particles in the system grows with a smaller exponent than the displacement of the first particle. Such a “dispersion” is obviously not possible in the case of a semi-infinite string since particles are coupled. Setting  $m = 1$  in the above expressions we recover known results for the ASEP.

In the unbiased case ( $\mu = 0$ ), the advance of the leading particle is expected to be ultra-slow and to follow the logarithmic scaling law characteristic of Sinai diffusion.

## 7. Discussion

As it was outlined in Ref. [19], the holes in the closed string with  $l = 1$  and with hop rates  $p_i, q_i$  can be regarded as large particles of size  $d = 2$  with hop rates  $\tilde{p}_i = q_{i+1}$ ,  $\tilde{q}_i = p_{i-1}$ . Although, for  $l > 1$ , a strict mapping between the two models does not exist, the phenomenological results obtained in this work show that the basic exponents  $\mu_1, \mu_2$  of the closed string with parameter  $l$  are related to the basic exponents  $\tilde{\mu}_1, \tilde{\mu}_2$  of an exclusion process with particles of size  $d = l + 1$  in the following way:  $\mu_1 = \tilde{\mu}_2, \mu_2 = \tilde{\mu}_1$ .

Comparing the exponent governing the decay of the steady-state current of a closed string to that of the ASEP, we see that the former is smaller for any  $\mu > 0$ , i.e. the coupling between particles facilitates the transport in this set-up. Moreover, the exponent decreases monotonously with  $l$  and finally tends to zero in the limit  $l \rightarrow \infty$ ‡. When not all particles are coupled with each other but they form finite  $m$ -strings, the coupling has the opposite effect: With increasing  $m$ , the transport slows down more and more compared to the ASEP both in the steady state and in the case of the invasion.

Contrary to the problem of invasion of uncoupled particles, in the case of a semi-infinite string, both the displacement of the head and the number of particles in the system grows obviously with the same power of time. This exponent is larger than that describing the increase of the number of particles in the ASEP if  $\mu > 1/2$ , meaning that the coupling is favourable in this case in the point of view of the bulk of particles. However, if  $\mu < 1/2$ , the inflow of particles is slowed down by the coupling. As far as the first particle is concerned, it diffuses faster in the ASEP if  $\mu > \mu_l^*$ , otherwise the diffusion exponents are equal in the two models. The influence of the parameter  $l$  on the transport shows a tendency similar to that in the closed string: The diffusion exponent increases monotonously with  $l$  (except of the regime  $\mu < \mu_l^*$ , where it is  $l$ -independent) and tends to 1 if  $l \rightarrow \infty$ .

The diffusion of the semi-infinite string can be speeded up by “pulling” the head of the string, that means when the first particle is not allowed to hop to the left. In this case, one can show that the time scale of overcoming a barrier is reduced from  $O(\tau)$  to  $O(\tau^{1/(l+2)})$ , which results in that the diffusion law in eq. (15) is valid in the entire

‡ We remind the reader that our results are valid in scaling regime  $\ln L \gg l$ .

biased phase  $\mu > 0$ . Comparing this model to the invasion of uncoupled particles, the diffusion of the pulled string is faster than that of the first particle in case of the ASEP only if  $\mu < \frac{l}{l+2}$ , while the inflow of particles is faster for the pulled string for any  $\mu$ .

Relaxing the hard-core exclusion condition in the ASEP, i.e. prescribing for the positions of consecutive particles the weaker condition  $x_i \leq x_{i+1}$  instead of  $x_i < x_{i+1}$ , we arrive at a zero-range process. Doing so for the model with coupled particles but keeping the attractive interaction  $x_{i+1} - x_i \leq l+1$ , we obtain a model which is no longer a ZRP. Due to the absence of hard-core repulsion, the high-density phase in the steady state of the closed string shrinks to the minimum in the largest trapping region, where a condensate forms and the low-density phase extends to the whole system. The current is thus expected to vanish as  $J_L \sim L^{-1/\mu_2} \sim L^{-\frac{1}{(l+1)\mu}}$ .

Finally, we mention that, as a possible generalisation of the model with limited inter-particle spacings, one could apply elastic pair-interactions by the help of which the crossover between the model with uncoupled particles (ASEP) and that studied in the present work could be investigated.

## Acknowledgments

This work has been supported by the National Office of Research and Technology under Grant No. ASEP1111.

## References

- [1] S. Alexander, J. Bernasconi, W.R. Schneider and R. Orbach, *Rev. Mod. Phys.* **53**, 175 (1981).
- [2] S. Havlin and D. Ben-Avraham, *Adv. Phys.* **36**,695 (1987).
- [3] W. Haus and K.W. Kehr, *Phys. Rep.* **150**, 263 (1987).
- [4] J.-P. Bouchaud and A. Georges, *Phys. Rep.* **195**, 127 (1990).
- [5] H. Kesten, M.V. Kozlov and F. Spitzer, *Compositio Math.* **30**, 145 (1975); F. Solomon, *Ann. Prob.* **3**, 1 (1975).
- [6] B. Derrida and Y. Pomeau, *Phys. Rev. Lett.* **48**, 627 (1982).
- [7] Ya.G. Sinai, *Theor. Probab. Appl.* **27**, 247 (1982).
- [8] P. Le Doussal, C. Monthus, and D.S. Fisher, *Phys. Rev. E* **59**, 4795 (1999).
- [9] F. Spitzer, *Adv. Math.* **5**, 246 (1970).
- [10] For a review, see: M.R. Evans and T. Hanney, *J. Phys. A* **38**, R195 (2005).
- [11] T.M. Liggett, *Stochastic Interacting Systems: Contact, Voter, and Exclusion Processes* (Springer, Berlin, 1999).
- [12] For a review, see: G.M. Schütz, in *Phase Transitions and Critical Phenomena*, vol. 19, edited by C. Domb and J.L. Lebowitz (Academic, San Diego, 2001), Vol. 19.
- [13] M.R. Evans, *Europhys. Lett.* **36**, 13 (1996).
- [14] R. Juhász, L. Santen, and F. Iglói, *Phys. Rev. Lett.* **94**, 010601 (2005).
- [15] R. Juhász, L. Santen, and F. Iglói, *Phys. Rev. E* **72**, 046129 (2005).
- [16] E. Koscielny-Bunde, A. Bunde, S. Havlin, and H.E. Stanley, *Phys. Rev. A* **37**, 1821 (1988).
- [17] G. Tripathy and M. Barma, *Phys. Rev. Lett.* **78**, 3039 (1997); *Phys. Rev. E* **58**, 1911 (1998).
- [18] J. Krug, *Braz. J. Phys.* **30**, 97 (2000).
- [19] R. Juhász, L. Santen, and F. Iglói, *Phys. Rev. E* **74**, 061101 (2006).
- [20] For a review, see: M. Barma, *Physica A* **372**, 22 (2006).
- [21] D. Chowdhury, L. Santen, and A. Schadschneider, *Phys. Rep.* **329**, 199 (2000).

- [22] D. Chowdhury, A. Schadschneider, and K. Nishinari, *Physics of Life Reviews* (Elsevier, New York, 2005), Vol. 2, p. 318.
- [23] D.K. Lubensky and D.R. Nelson, *Phys. Rev. E* **65**, 031917 (2002).
- [24] Y. Kafri, D.K. Lubensky, and D.R. Nelson, *Biophys. J.* **86**, 3373 (2004).
- [25] J. Howard, *Mechanics of Motor Proteins and the Cytoskeleton* (Sinauer, Sunderland, 2001).
- [26] T. Harms and R. Lipowsky, *Phys. Rev. Lett.* **79**, 2895 (1997).
- [27] For a review, see: F. Jülicher, A. Ajdari, and J. Prost, *Rev. Mod. Phys.* **69**, 1269 (1997).
- [28] I. Derényi and T. Vicsek, *Phys. Rev. Lett* **75**, 374 (1995).
- [29] Z. Csahók, F. Family, and T. Vicsek, *Phys. Rev. E* **55**, 5179 (1997).
- [30] T. Antal, P.L. Krapivsky, and K. Mallick, *J. Stat. Mech.* P08027 (2007).
- [31] R. Pei, S.K. Taylor, D. Stefanovic, S. Rudchenko, T.E. Mitchell, and M.N. Stojanovic, *J. Am. Chem. Soc.* **128**, 12693 (2006).
- [32] J.-P. Bouchaud, A. Comtet, A. Georges, and P. Le Doussal, *Ann. Phys.* **201**, 285 (1990).
- [33] H. Kesten, *Acta Math.* **131**, 207 (1973).
- [34] R.A. Blythe, M.R. Evans, F. Colaiori, and F.H.L. Essler, *J. Phys. A: Math. Gen.* **33**, 2313 (2000).
- [35] J. Galambos, *The Asymptotic Theory of Extreme Order Statistics* (John Wiley and Sons, New York, 1978).
- [36] K.P.N. Murthy and K.W. Kehr, *Phys. Rev. A* **40**, 2082 (1989).